Experimental testing of a hybrid sensible-latent heat storage system for domestic hot water applications

Andrea Frazzica [a,*], Marco Manzan [b], Alessio Sapienza [a], Angelo Freni [a], Giuseppe Toniato [c], Giovanni Restuccia [a]

[a] CNR – Istituto di Tecnologie Avanzate per l'Energia "Nicola Giordano", Via Salita S. Lucia sopra Contesse 5, 98126 Messina, Italy
[b] Dept. of Engineering and Architecture, University of Trieste, Trieste, Italy
[c] Riello S.p.A., Via Ing Pilade Riello 7, 37045 Legnago (VR), Italy

HIGHLIGHTS

- Experimental characterization a small scale heat storage for domestic applications.
- The heat storage is based on the hybrid "sensible + latent" configuration.
- Two different PCMs were compared, namely, a commercial paraffin and a hydrate salt mixture prepared in lab.
- A heat storage density increasing up to 13% has been highlighted.
- A new ESP-r component has been developed and validated thanks to the experimental outcomes.

ARTICLE INFO

Accepted 26 September 2016

Keywords:
PCM
Heat storage
Domestic hot water
ESP-r
Hybrid heat storage

ABSTRACT

Aim of this work is to present the results of the testing of a small scale hybrid sensible/latent storage system (nominal volume 48.6 dm^3), consisting of water in which macro-encapsulated phase change materials (PCMs) are added. Two different PCMs were macro-encapsulated, a commercial paraffin and a hydrate salts mixture prepared in the CNR ITAE lab, and loaded inside the tank in order to be tested. Different volume ratios between the PCM and the water were tested. The tests were conducted simulating different domestic hot water draw-off profiles.

The resulting data showed an appreciable increase of heat storage capacity per unit of volume, even for limited fractions of PCM employed, reaching up to 10% of heat storage increasing by 1.3 dm^3 of hydrate salts mixture added. Finally, the experimental results were used to test a numerical method of a PCM enhanced tank for dynamic plant simulations in ESP-r environment.

1. Introduction

Currently, the development of innovative heat storage systems represents one of the main issues to be overcome, in order to promote the market penetration of renewable energies as well as to optimize the energy management, especially for application in residential buildings [1].

The state of the art of commercially available heat storages for domestic applications is dominated by sensible systems [2], based on water as heat storage medium. Actually, for applications at temperatures lower than 100 °C, the sensible/water system seems to be the best option thanks to its availability, its low cost, and sufficiently high specific heat [3]. Nevertheless, it suffers of the intrinsic limit related to the heat losses to the ambient that causes reduction of energy stored during the stand-by periods. This leads to the necessity of careful insulation of the vessels, thus reducing the overall volumetric heat storage density of the systems.

During last years, application of Phase Change Materials (PCMs) as heat storage mediums has been proposed in order to increase the heat storage density as well as to guarantee an optimization of the performance achievable by systems exploiting renewable energy sources [4,5]. To this aim, initially, many efforts have been dedicated to the development of advanced materials with increased heat storage capacity, good heat transfer properties and excellent cycling stability [6]. Actually, these research activities have led to excellent results, which are confirmed by the growth of new companies commercializing PCMs for heat storage applications [7,8].

* Corresponding author.
E-mail address: andrea.frazzica@itae.cnr.it (A. Frazzica).

Nomenclature

Cp	specific heat [kJ/(kg K)]
E	energy [kJ]
$\dot{m}$	flow rate [kg/s]
t	time [s]
T	temperature [°C]
$u(P)$	uncertainty on power calculation [kW]
V	volume [m^3]
ρ	density [kg/m^3]

Subscripts

disch	discharge
nom	nominal
tap	tap water
user	user
w	water

Recently, more attention has been paid to the realization of advanced heat storage concepts, based on the employment of PCMs [9]. In case of heat storage for domestic applications, two main approaches have been followed namely, the integration of macro-capsules inside a water heat storage container [10,11] and the realization of full scale heat storages based on PCM embedded inside efficient heat exchangers [12–14]. Despite the higher storage volumetric density achievable by the latter one, the low delivered thermal power during discharging phase represents its main limit [15]. This is mainly due to the slow kinetic of phase transition as well as the poor thermal conductivity of PCMs [11]. In order to overcome this limit, different approaches have been proposed in literature, like the addition of carbon powders [16] or the embedding of PCM inside open-cell metal foams [17], to increase the overall thermal conductivity of the material. Although the obtained results seem encouraging, these approaches are limited by the high cost of the employed materials as well as the complicated preparation procedure. Another possible solution recently proposed for thermal energy storage for domestic applications, is to exploit supercooled state of particular PCMs, such as Sodium Acetate Trihydrate, to increase heat storage capacity limiting the heat losses through the environment. Recent experimental results [18] demonstrate the interesting achievable performance of this innovative concept. Nevertheless, some issues like material stability and reliability of the supercooling process need to be carefully investigated to make this approach more attractive.

In such a background, the approach based on the inclusion of certain quantities of macro-encapsulated PCMs inside a water tank, despite the lower increasing in thermal storage density, is not affected by limitations in discharging power, since water is the primary heat transfer medium [10]. Moreover, it results to be a more cost effective solution. Some examples have been proposed within the activities of IEA Task 32 "Advanced storage concepts for solar and low energy buildings" [19]. In that case, configurations employing metallic bottles filled with organic as well as inorganic PCMs, whose thermal conductivity was increased by means of graphite filler, were experimentally investigated. The results confirmed the possibility of increasing heat storage density, compared to water. Nevertheless, the low heat transfer surface to volume ratio of the employed macro-capsules limited the achievable charging/discharging rate. Castell et al. [20] have reported similar results.

Accordingly, such a kind of configuration needs to be optimized in order to exploit as much as possible the benefit deriving from the PCMs implementation.

Furthermore, numerical analysis carried out by means of software for energy systems simulation, like ESP-r, can be a useful tool to analyze application of PCM in buildings. By analyzing literature, only few examples are available due to the lack of validated components. For instance, in [21] analysis of PCM embedded in the gypsum panels to store solar energy thus reducing the thermal load in buildings has been carried out thanks to the implementation of a dedicated component model in ESP-r. More recently, Padovan and Manzan [22] have optimized a hybrid sensible/latent heat storage in ESP-r environment, but no experimental validation has been reported so far.

Accordingly, aim of the present paper is the experimental analysis of a domestic small-scale heat storage based on the hybrid "sensible + latent" configuration properly sized for space heating and DHW delivering. Sensible configuration has been experimentally compared to the hybrid ones. Two different PCMs, never investigated in literature under relevant operating conditions, have been integrated inside the heat storage by macro-encapsulating them in sealed parallelepiped polymeric capsules. In particular, the employed PCMs are a commercial paraffin and a hydrate salt mixture prepared at the CNR ITAE lab. The effect of varying volume of PCM inside the heat storage has been experimentally analyzed by means of a properly designed and realized test rig, able to simulate the daily hot water withdrawal profiles. Finally, a new ESP-r component, able to simulate the behavior of a hybrid heat storage, has been defined, implemented and validated by means of the obtained experimental data. This will cover the lack of available components to simulate the behavior of PCM-based heat storage for system simulation.

2. Tested heat storage and test rig

With the aim to evaluate the performance of a hybrid "sensible + latent" heat storage for domestic application, a cylindrical vertical tank has been realized. It is a fully mixed system (without internal heat exchangers) made of stainless steel, and its main geometrical characteristics are reported in the following Table 1.

It has been realized with the idea to get a tank as flexible as possible in order to vary different testing parameters like typology, amount and position of PCM material and to monitor temperatures of several points within the tank and inside PCM macro-capsules.

Fig. 1 shows the realized cylindrical storage, in which the different available hydraulic connections and the thermocouples feedthroughs can be recognized. Furthermore, the allocation of the six thermocouples inside the tank (T0–T5), the thermocouple for PCM (T7), the position of the PCM module and the inlet and outlet water connections are reported. They allow the monitoring of the temperature evolutions along the vertical axis of the tested

Table 1
Main geometrical characteristics of the tank.

Nominal volume [dm^3]	48.6
Height [m]	0.85
Diameter [m]	0.27
Weight [kg]	35.6

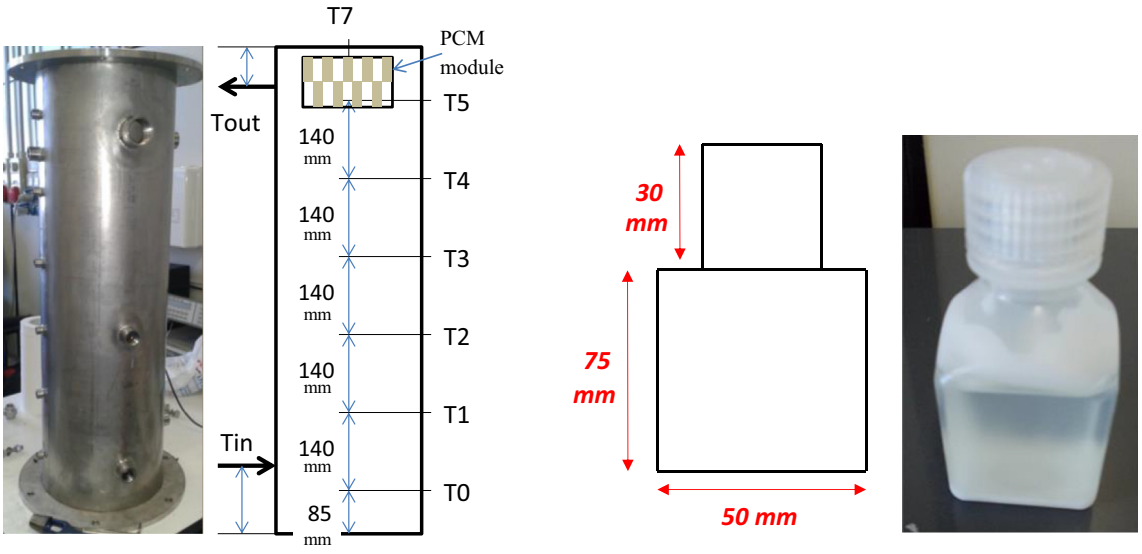

Fig. 1. Picture of the realized vertical heat storage, before thermal insulation and the schematic of the allocation of the thermocouples inside the tank (on the left-hand side); schematic of the macro-capsule employed and its dimensions (on the right-hand side).

storage, in order to verify the presence of stratification effects. On the right-hand side of Fig. 1, a schematic of the employed macro-capsules and its picture are reported. They are made of polypropylene, with a square-based parallelepiped geometry and a sealed cap. The reduced dimensions of the capsules have been selected in order to enhance the heat transfer between the PCM and the surrounding water, thanks to the high heat transfer surface to volume ratio, thus guarantying to achieve high charging/discharging power.

In order to test the heat storage, a test rig was specifically designed and built in the CNR ITAE laboratories. It was realized in accordance to the specifications reported from the standard EN 12977-3 [16], accordingly, it allows to carry out all the specified tests for the full characterization of a domestic hot water storage. Moreover, it can be employed for the simulation of different draw-off profiles, typical of domestic applications (e.g. simulation of taking a shower, etc.).

Fig. 2 reports the hydraulic schematic of the test rig. It is made of two sections, the one at high temperature for energy providing, and the one at low temperature for energy withdrawal. In the same figure, the main components of the rig are also represented: the HEX for the connection to the electric boiler (24 kW heating power); the high temperature heat storage tank, which is necessary in order to get a driving temperature as much constant as possible, by smoothing the power peaks during charge phases; the tested heat storage, connected both to the heating source and to the energy withdrawal side; an external HEX, to connect the tested heat storage to the energy withdrawal side, avoiding potential water contamination in case of leakages from PCM capsules; an automatic mixing valve, which allows setting the temperature delivered to the user during the discharging phase.

In Fig. 3, the built test rig is shown. It is fully automatized, by means of National Instruments data acquisition and management system, which is connected to a Labview software able to drive

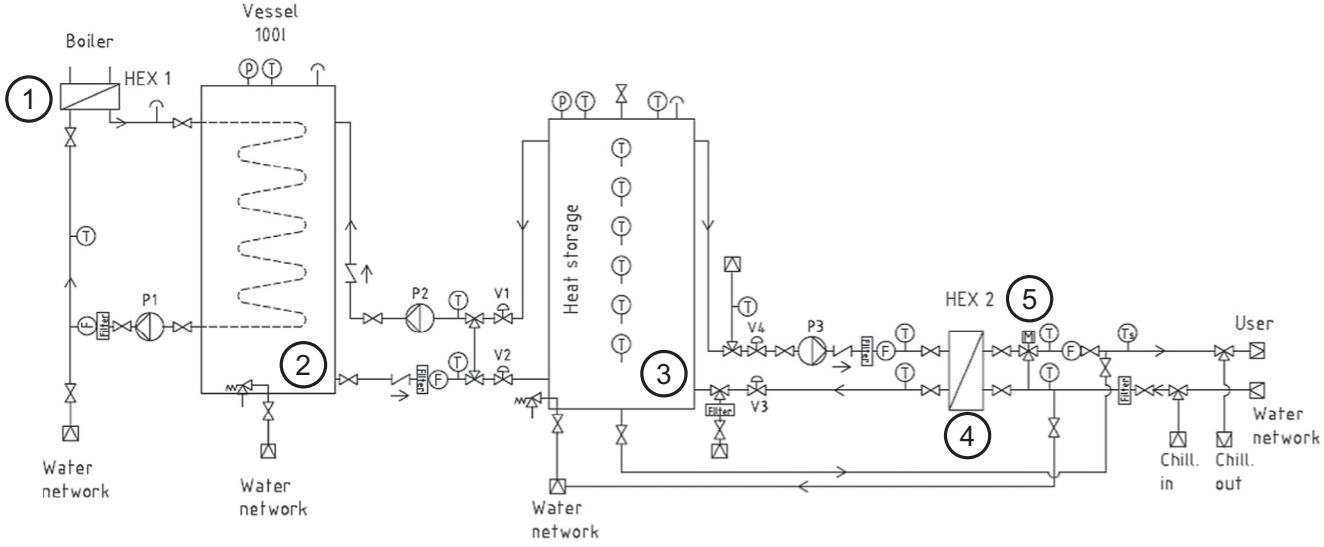

Fig. 2. Hydraulic layout of the realized test rig: (1) heat exchanger connected to electric boiler, (2) high temperature buffer heat storage, (3) heat storage under testing, (4) intermediate heat exchanger between heat storage side and user side, (5) automatic mixing valve.

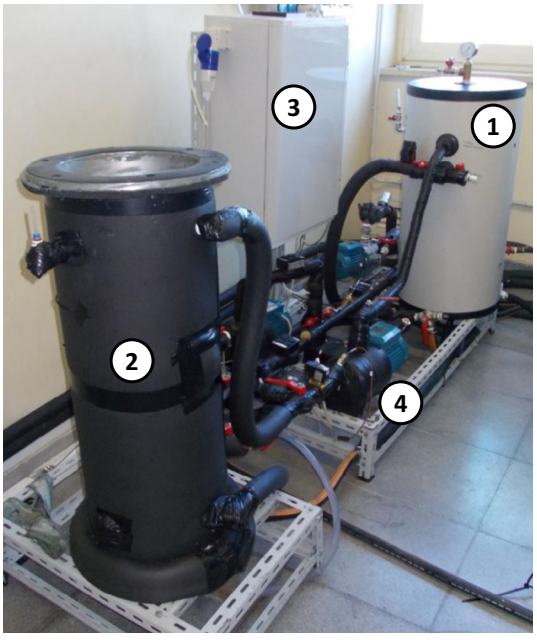

Fig. 3. Picture of the installed test rig at the CNR ITAE laboratory: (1) high temperature buffer heat storage, (2) heat storage under testing, (3) control and management unit, (4) hydraulic circuit for charging and discharging phases simulation.

all the electric valves and pumps and to acquire all the needed data for the evaluation of the heat storage performance (temperatures and heat flows).

Particular attention has been dedicated to the selection of proper sensors. The temperature is measured by means of thermocouples "type T" (characterized by an accuracy of ±0.5 °C), while the flow rate is measured by means of an ultrasonic sensor, able to work with different kind of fluids, having a measuring range between Q_{min} = 0.01 dm^3/s and Q_{max} = 1.66 dm^3/s (CONTECA® ULTRA). The measuring error curve of the flow sensor shows an error, in the measuring range, of about 1% of the measured value.

Starting from the metrological characteristics of the employed sensors, an analysis of the experimental error has been done, according to the international standards [25]; the error on the power measurement can be computed by the following expression:

$$u(P) = \sqrt{\left[(C_P \times \Delta T) \times \frac{0.01 \times \dot{m}}{\sqrt{6}}\right]^2 + \left[(\dot{m} \times C_P) \times \frac{0.5}{\sqrt{3}}\right]^2} \quad (1)$$

where $u(P)$ [kW], represents the uncertainty, Cp [kJ/(kg K)] the fluid specific heat, ΔT [K], the measured temperature difference across each component and $\dot{m}$, kg/s, the mass flow rate. Of course, this value changes sensibly with the testing conditions. In general, especially during the discharging phases, thanks to the high employed flow rate and temperature difference measured, an experimental error around 3% was calculated for discharging power. The calculated error on the discharged energy was around 5%.

3. Experimental activity

The experimental activity on the heat storage was divided in two different phases: the first one aimed at the characterization of the sensible heat storage as reference system, the second one to the evaluation of the achievable performance by hybrid storage made of water and PCM, employing different kind and amount of PCMs.

3.1. Sensible heat storage

The characterization of the sensible heat storage, employing water as heat storage medium, has been carried out following the specifications reported in the standard EN 12977-3 [24] for the "fully mixed" tank configuration. In particular, in order to evaluate the heat loss capacity rate, U, the heat storage was charged at 70 °C and then let cooling down by releasing heat to the ambient maintained at temperature around 25 °C. While, to determine the actual heat storage volume, V_{real}, both charging and discharging phases were performed according to the recommendations reported in the standard [24]. Table 2 summarizes the employed testing conditions.

In Table 2, conditioning phase consists of bringing the entire heat storage at uniform temperature before starting the charging phase, in order to avoid internal temperature gradients.

Once obtained the experimental data, as requested by the standard test procedure, the values have been fitted by means of a reliable numerical model able to simulate the performance of a fully mixed heat storage. To this aim, the Type 60, available in the libraries of the TRNSYS 17 software [18] was employed as standard. Accordingly, a data regression was performed both for stand-by cooling down and charging/discharging in order to minimize the deviation, by varying the free parameters: U and V_{real}. Following Fig. 4 summarizes the obtained results.

As reported in Fig. 4, the actual heat storage volume was slightly lower (3.6%) than the nominal one, reported in Table 1. This is related to issues occurring during tank realization phase; nevertheless, this limited deviation confirms that the measured data are consistent with the ones deriving from the standard characterization. Concerning the heat loss capacity rate, generally, the obtained value, 2.05 W/K, is in line with common data available in literature [27], which confirms that the installed insulation is reliable.

3.2. Hybrid sensible + latent heat storage

Aiming at the comparison of the performance of the different storage configurations realized, two more tests have been applied as suggested by de Gracia et al. [23]:

- Test A, consisting in a continuous discharge of the heat storage, which is completed once that the temperature delivered to the user falls below 35 °C. Subsequently, there is a stand-by period ranging between 45 and 60 min, during which, in presence of PCM, there could be a reheating process. Then, another discharging phase is performed. The process is repeated until the heat storage is not able to deliver water to the user with a temperature at least of 35 °C.

Table 2
Performed tests according to the standard EN 12977-3, for the main storage parameters characterization [24].

Phase	Duration	Flow rate [kg/s]
Stand-by cooling down test		
Conditioning	Up to 25 °C	0.012–0.017
Charging	Up to 70 °C	0.012–0.017
Stand-by	30 h	0
Charging/discharging test		
Conditioning	Up to 25 °C	0.012–0.017
Charging	Up to 70 °C	0.012–0.017
Discharging	Down to 25 °C	0.012–0.017

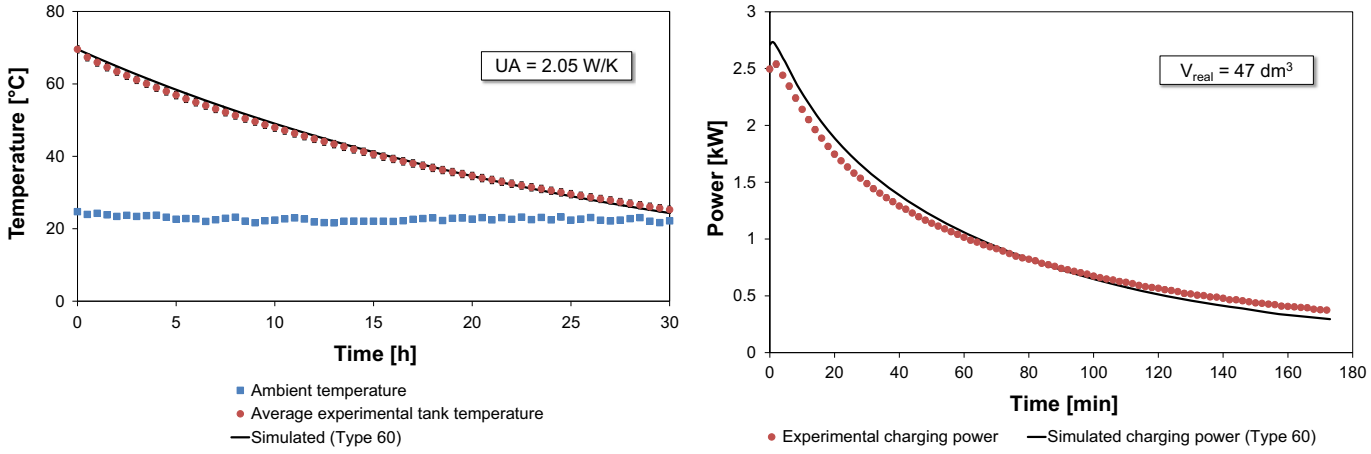

Fig. 4. Stand-by cooling down process fitted by TRNSYS simulation, on the left-hand side, and charging experimental evolution with the relative fitting, on the right-hand side.

- Test B, is similar to the test A, but consists of different withdrawals of the duration of 5 min each, with an interval ranging between 45 and 60 min between two consecutive withdrawals. In addition, in this case, the process is repeated until the storage is able to deliver hot water at 35 °C.

As the aim was to simulate a real user, the mass flow rate during discharging phases has been selected accordingly, with values ranging between 0.13 and 0.16 kg/s, typical of domestic users.

The comparison was carried out employing two different PCMs, which have been selected to be included inside the tank, namely:

- PCM 58, a mixtures of hydrates salts, $Mg(NO_3)_2{\cdot}6H_2O$ and $MgCl_2{\cdot}6H_2O$ at the eutectic composition 58.7–41.3%, prepared at the CNR ITAE laboratories employing proper stabilizing agents [28].
- RT 65, an organic compound produced by the company Rubitherm [7].

The materials have been chosen considering a heat storage for domestic applications to be coupled to solar thermal collectors as well as to other appliances like gas boiler or micro-CHP.

Their main thermodynamic characteristics were measured in laboratory by means of specific apparatuses: Mettler Toledo DSC 27HP for latent heat and melting temperature evaluation, Mathis TCi for thermal conductivity measurements, similarly as reported in [29]. Table 3 summarizes the results of the measurements.

Afterwards, the following heat storage configurations have been tested.

- Sensible heat storage (SENSIBLE);
- Hybrid sensible + latent employing 1.3 dm^3 of RT 65 (RT 65 CONFIG 1);
- Hybrid sensible + latent employing 2.25 dm^3 of RT 65 (RT 65 CONFIG 2);
- Hybrid sensible + latent employing 1.3 dm^3 of PCM 58 (PCM 58 CONFIG).

Table 3
Thermodynamic properties of the employed phase change materials (PCMs).

	PCM 58	RT 65
Melting T [°C]	57.7	65.8
Latent heat [kJ/kg]	105	152
Specific heat solid state [kJ/(kg K)]	2.8	2
Density solid state [kg/m^3]	1800	880
Thermal conductivity solid state [W/(m K)]	1.3	0.2

The selection of the macro-capsules has been performed in order to employ cost effective materials, with proved resistance to possible corrosive effects and with good thermal stability at the working temperatures. Moreover, in order to increase the heat transfer area between PCM and water, the volume of each capsule has been limited to 80 cm^3. The final selection was oriented to polypropylene macro-capsules with a parallelepiped geometry, employing a sealing system able to avoid leakages of PCM in liquid phase, as reported in Fig. 1.

After preparation of the right number of PCM capsules, they were introduced into the tank by means of a properly designed container, which allowed the allocation at the desired height during the execution of the tests.

Finally, both test A and test B were repeated for each heat storage configuration as reported in Table 4.

Test A and B have been performed for all the selected configurations, varying the charging temperature, in order to comparatively evaluate their performance. On the contrary, the stand-by cooling down test has been replicated only for SENSIBLE and PCM 58 CONFIG, aiming at the analysis of the effect related to the presence of PCM inside the tank.

In the following sections, the results of the experiments are analyzed in detail.

3.3. Stand-by cooling down test

As already stated above, the stand-by cooling down test, which is necessary to characterize the sensible heat storage according to the standard, has been also repeated for the hybrid "sensible + latent" heat storage configuration employing PCM 58. It has been performed to analyze the effect under these working conditions of the PCM inclusion. Fig. 5 reports both charging and stand-by phases measured.

Fig. 5a reports the charging phase evolution both for SENSIBLE and PCM 58 CONFIG. This case has been selected to analyze the charging dynamics thanks to the low flow rates employed (less than 0.02 kg/s), which allow to highlight the different behavior between the two systems. First, due to experimental issues, it has to point out that the charging flow rates employed for the two configurations are quite different, as reported in Table 4, which causes a longer charging period for the SENSIBLE than for the PCM 58 CONFIG, to reach the same temperature of 70 °C,

Table 4
Performed tests for the comparative evaluation of the tested heat storages.

Configuration	Test	Charging T [°C]	Charging flow rate [kg/s]	Discharging medium	Discharging flow rate [kg/s]
SENSIBLE	Stand-by cooling down	70	0.012	–	–
	Test A	62–74	0.2–0.22	Tap water	0.13–0.14
	Test B	64–70	0.2–0.22	Tap water	0.13–0.14
RT 65 CONFIG 1	Test A	69–75	0.2–0.22	Tap water	0.13–0.15
	Test B	67–73	0.2–0.22	Tap water	0.14–0.15
RT 65 CONFIG 2	Test A	65–71	0.2–0.22	Tap water	0.12–0.15
	Test B	66–73	0.2–0.22	Tap water	0.13–0.14
PCM 58 CONFIG	Stand-by cooling down	70	0.018	–	–
	Test A	61–70	0.2–0.22	Tap water	0.13–0.15
	Test B	62–72	0.2–0.22	Tap water	0.13–0.16

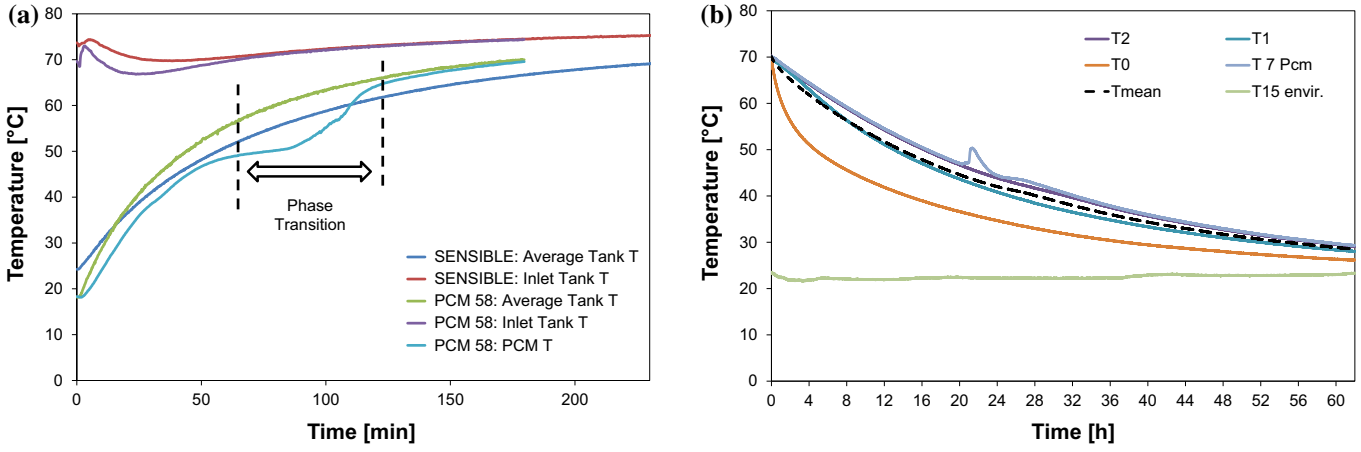

Fig. 5. (a) Main process temperatures evolution during low flow rate charging phases for SENSIBLE and PCM 58 CONFIG; (b) Measured temperatures inside the heat storage during the stand-by cooling down phase.

making them difficulty comparable. The inlet temperature for both the tests is maintained sufficiently constant, thanks to the presence of the buffer heat storage on the test rig. This means that the simulated charging phases can be considered as a typical heat storage connected to a heating device able to deliver a quasi-constant temperature (e.g. gas boiler, micro-CHP). Looking at the experimental evolutions of the temperatures inside the tank of the PCM 58 CONFIG, it is evident that there is a phase transition around the nominal melting temperature, 58 °C, which causes a high deviation of the PCM temperature from the average tank temperature. What is interesting to analyze is the behavior of the system during the two sensible heating phases, namely, before and after phase transition. In fact, at low temperature, when the PCM is in the solid state, there is always an evident temperature difference between the water temperature and PCM temperature (which is measured in the middle of the capsule). This is caused by the fact that, in this phase, the dominant heat transfer mechanism is the thermal conduction. Accordingly, the poor thermal conductivity, typical of these materials, heavily affect the process. On the contrary, once that the melting point is reached, the main heat transfer mechanism become the convection, which noticeably enhance the overall heat transfer coefficient, thus guarantying a quick reduction of the temperature difference between water and PCM. This represents a first interesting conclusion, since, if on one hand the inclusion of high thermal conductivity materials inside the PCM allows better performance when the material is in the solid state, on the other hand, the presence of different phases inside the capsule could limit the convection phenomena lowering the overall PCM heat transfer performance in the liquid phase.

Fig. 5b depicts the temperatures evolution inside the tank in PCM 58 CONFIG during the stand-by period. The reported temperatures are recorded along the longitudinal axis of the heat storage, as represented in Fig. 1. First, it is evident that, despite the small dimension of the heat storage, there is still a certain degree of stratification inside, thanks to its high height-to-diameter ratio. The stratification is probably affected by the presence of the PCM macro-capsules. Indeed, while the two thermocouples at the bottom of the tank, T0 and T1, shows a faster cooling down process, the thermocouples located closer to the PCM container tend to maintain a more similar temperature. In particular, looking at the Fig. 5b, the phase transition is well highlighted by the evident sub-cooling that affects the material. Actually, the solidification starts only at a temperature around 48 °C, and then, the exothermic reaction causes an increasing of temperature inside the material itself.

3.4. Test A

As reported in Table 4, several Tests A have been performed on the four identified configurations. The main aim was to analyze the evolution of internal temperatures during the imposed withdrawal profile, comparing the results obtained by different configurations and, finally, evaluating the different energies delivered to the user.

Fig. 6a reports, as example, the dynamic evolution of the temperatures monitored inside the tank during the Test A for RT 65 CONFIG 2. In order to understand the recorded temperature evolutions it has to be pointed out that the discharging process is performed by withdrawing hot water from the top of the tank and

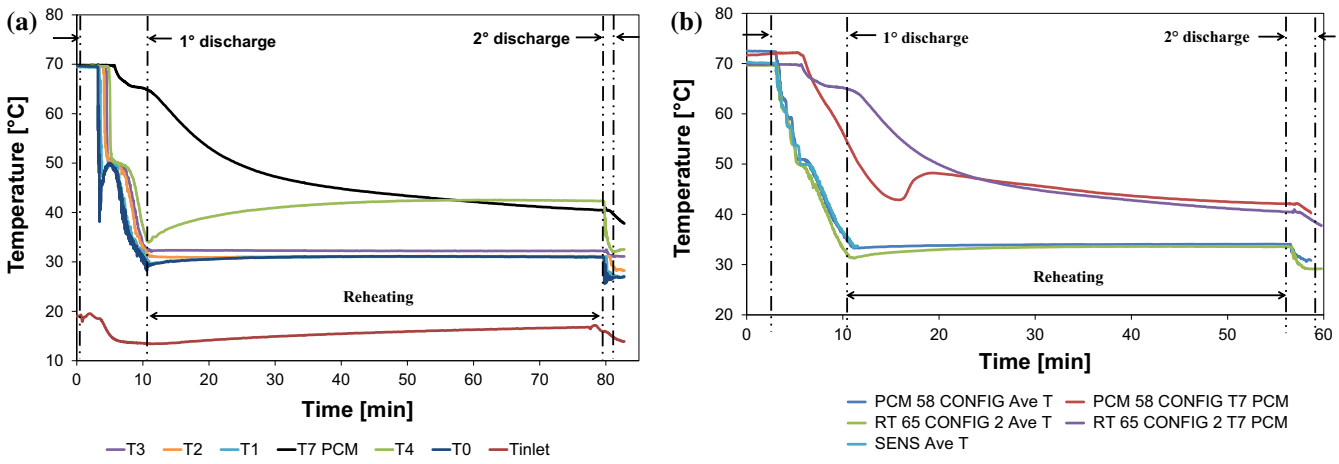

Fig. 6. (a) Temperature evolutions inside the tank during a Test A discharging phase for the RT 65 CONFIG 2; (b) comparison between experimental evolutions of average tank temperature and PCM temperature under comparable boundary conditions for PCM 58 CONFIG, RT 65 CONFIG 2 and SENSIBLE.

sending back the colder water to the bottom of the tank. The water is cooled down through the intermediate heat exchanger, see Fig. 2, by exchanging heat with the tap water flowing on the user side. Having in mind this, the temperature evolutions showed in Fig. 6a can be explained. Indeed, during the first part of the discharging process, the temperature of the water withdrawn from the top of the tank is constant, because the cold water entering at the bottom of the tank pushes the hot water upward. Accordingly, in this phase the intermediate heat exchanger works in a steady state conditions, indeed the entering temperatures both on the heat storage and user side are constant. This means that the cooled water coming back to the tank is also at constant temperature, which, in the case reported in Fig. 6a is about 50 °C. Once that the cold water reaches the top of the heat storage, the hot temperature delivered to the heat exchanger suddenly drops down, causing a sort of plateau recorded inside the tank, reaching a sort of fully mixed system condition. Subsequently, the temperatures inside the tank starts again to go down. The withdrawal is stopped once that the temperature delivered to the user falls below the 35 °C.

During this phase, the PCMs start to solidify when the temperature of the surrounding water drops down to 50 °C. Thanks to the high flow rate of the exchanged water and to the high temperature difference between PCM and water, the heat transfer is enhanced, so the phase transition results quite fast. When the system is in stand-by, after the first discharge, as expected, the PCMs tend to heat up the surrounding water, thus guarantying a reheating of the water itself. This affects only the upper zone of the heat storage. In particular, in this case, a reheating of about 10°C has been registered. Accordingly, the tank has been able to deliver again hot water to the user for a duration of about 2 min.

Fig. 6b compares three different configurations subjected to Test A: SENSIBLE, RT 65 CONFIG 2 and PCM 58 CONFIG. In this case, only the average temperatures and the PCM temperatures are reported. Looking at the average temperatures recorded, what is particularly interesting is that the discharge durations for the different configurations are similar. This allows to conclude that the inclusion of PCMs inside the tank does not affect the discharging performance, or, in other words, that the discharging power is similar in each configuration. Clearly, the presence of the PCM plays a role in the possibility of reheating the water, thus performing more discharging phases, as showed in Fig. 6b.

Moreover, the PCM temperature evolutions confirm the completely different behavior of the selected PCMs. Indeed, while the RT 65 undergoes a typical phase transition, which is clearly indicated by the temperature plateau around its nominal melting temperature, the PCM 58 suffers of an evident sub-cooling effect, which causes the shifting of the phase change process to a lower temperature.

3.5. Test B

Fig. 7 reports the evolution of internal tank temperatures during a Test B performed on the PCM 58 CONFIG. In this case the discharging phases have a duration of 5 min each. Again, the evolution of internal temperatures follow the one already analyzed for Test A. Thanks to the reheating process, the system in this configuration is able to perform three different discharging phases. Moreover, looking at the PCM temperature evolution, after the first discharging phase the material remains in the liquid state, simply delivering heat to the surrounding water during the first stand-by phase. The phase transition occurs only during the second discharging phase, again showing a clear sub-cooling effect.

4. Performance evaluation

In order to compare the experimental results obtained by testing the different configurations, the amounts of energy delivered to the user both during Test A and Test B have been evaluated, according to the following Eq. (2).

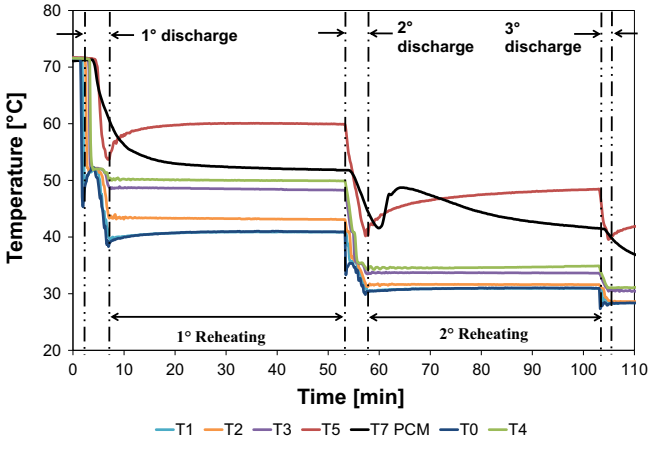

Fig. 7. Temperature evolutions inside the tank during a Test B discharging phase for the PCM 58 CONFIG.

$$E_{user} = \sum_{i=1}^{n} \int_{0}^{t_{disch}} \dot{m} Cp_w (T_{user} - T_{tap}) dt \quad (2)$$

where E_{user} [kJ], represents the energy delivered to the user during the discharging process, n, represents the number of performed useful discharges; t_{disch} [s], the duration of each discharge phase, $\dot{m}$ [kg/s], the discharging flow rate, Cp_w [kJ/kg K], specific heat of water, T_{user} [°C], measured temperature delivered to the user, T_{tap} [°C], measured tap water temperature.

Fig. 8 compares discharging powers and the relative integrated energies for three configurations, SENSIBLE, RT 65 CONFIG 2 and PCM 58 CONFIG, during a typical Test A. As already argued in previous paragraphs, the discharging powers during the first stage are comparable, oscillating around 14 kW. This confirms one more time that the system, even in presence of PCM, does not lose its dynamic performance. Accordingly, the energy discharged after the first discharging stage is almost the same for each configuration. After the stand-by period, there is again a brief discharging phase for the configurations employing PCM, characterized by lower power, about 12 kW, due to the lower temperature of the water inside the heat storage. This additional discharging phase allows increasing the total energy delivered to the user by the PCM-based systems.

Moreover, starting from the energy delivered to the user, an equivalent amount of DHW/space heating water produced has been calculated, according to the following Eq. (3):

$$V_{user} = \frac{E_{user}}{\rho_w Cp_w (T_{nom\_user} - T_{nom\_tap})} \quad (3)$$

where V_{user} [m^3], represents the equivalent hot water delivered to the user. ρ_w [kg/m^3], is the water density. T_{nom_user} [°C], is the nominal temperature to be delivered to the user both for DHW and low temperature space heating distribution systems (e.g. radiant panels) which is fixed at 40 °C. T_{nom_tap} [°C], is the average seasonal tap water temperature, fixed at 15 °C: This evaluation is necessary in order to avoid the influence related to the fluctuation of inlet tap water temperature registered during experimental testing.

Fig. 9 reports the equivalent water volume delivered to the user as function of the initial temperature inside the heat storage, registered under Test A conditions. The base line is represented by the sensible heat storage. The water volume delivered employing 1.3 dm^3 of RT65 (RT 65 CONFIG 1) is only slightly higher than the reference value. On the contrary, both the RT CONFIG 2 and PCM 58 CONFIG guarantee a remarkable enhancement of the volumetric heat storage capacity, about 10% respect to water. Of course, this increasing is more accentuated for charging temperatures only slightly higher than the nominal melting temperature of the employed PCM.

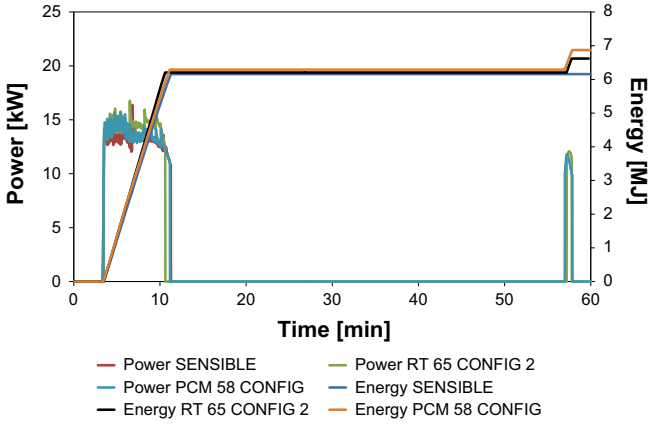

Fig. 8. Discharging powers and energies recorded during Test A for SENSIBLE, RT 65 CONFIG 2 and PCM 58 CONFIG.

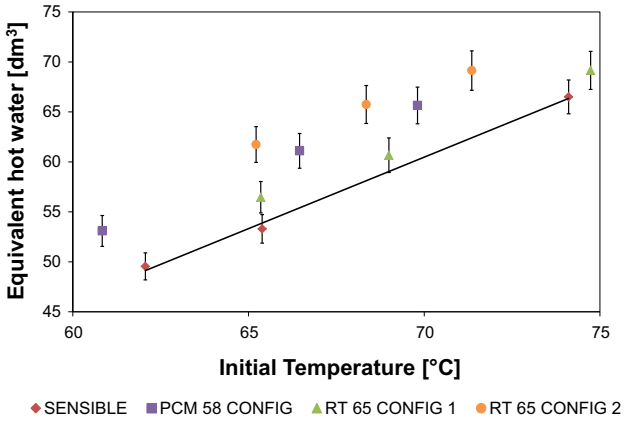

Fig. 9. Comparison between the equivalent water delivered to the user for all the tested configurations under Test A conditions.

What is of particular interest is the possibility of reaching almost the same results employing about half volume of PCM 58 respect to the RT 65. These outcomes are related to the higher density of the hydrates salt, which, on volumetric basis, presents a latent heat almost double if compared with the commercial organic compounds. Moreover, the highlighted sub-cooling effect in PCM 58 seems to have a reduced effect on the overall achievable performance of the system.

Similar results have been obtained for Test B, which means that the overall achievable performance by the tested configurations are only slightly influenced by the discharging conditions.

5. Numerical simulation

The correct exploitation of renewable resources, or the use of alternative heating systems such as cogeneration or trigeneration, requires an accurate design of sometimes-complicated systems. Nowadays dynamic simulation tools allow studying plant systems and plant/building coupling in different conditions. However, plant components should be modelled with accurateness and an experimental validation is always suggested. Tanks or energy storage systems are common components used in water system plants and a numerical model has been developed at the University of Trieste to simulate the effect of PCM to enhance thermal energy storage capabilities.

The experimental results are a precious asset for testing numerical models; therefore, the same tests have been carried using the developed code specifically designed for the code ESP-r [30]. The model features PCM filled cylindrical modules in vertical position. The model is a direct extension of a stratified tank component already present in ESP-r base code and has been extensively presented by Padovan et al. [31, 15ter]. Performance comparisons have been carried out for both the sensible and latent heat storage system.

5.1. Storage model

Esp-r stratified tank model features up to 100 water layers; a mixing algorithm is present in order to mix tank layers that features temperature inversion that is when the temperature of a layer is higher than the one of a higher layer. When, during a simulation, this situation occurs, for example due to cold-water injection at a low inlet port, the layers are mixed until no inversion is encountered.

The only component used for simulation is the tank avoiding the simulation of the heat exchangers present in the experimental test rig, therefore the available data are temperature and mass flow rate of water at the inlets and outlets of the tank, comparing the temperatures obtained at different levels as reported in Fig. 1.

In comparing numerical and experimental results however some different conditions should be taken into account. In the model the PCM modules are vertical cylinders, the user defines the module diameter, height and vertical position from the bottom of the tank. In the test rig, the PCM is contained in macro-capsules with a parallelepiped geometry and furthermore, the capsules are randomly positioned in a basket, as presented in Fig. 1, therefore the numerical model is able to simulate the latent heat effect on water tank temperature, but it is not possible to perform directly a comparison on PCM temperatures.

Now, numerical model is not able to consider sub-cooling effects, therefore, the comparison has been performed for RT65 PCM only. An additional issue arises for the comparison for short time periods when inverse gradient temperatures can develop. As stated before the tank model resolves immediately such situations by mixing the inverse temperature layers, this behavior is consistent with long time simulations, but can prevent an accurate representation in a short time scale. The tank model adopted is one-dimensional that is the temperature can change in vertical direction only, so local effects due to inlet jets cannot be simulated and plume formations cannot be simulated. This problem is shared with similar other models used in simulation systems such as TRNSYS [26], and it is difficult to overcome since it would require the use of CFD codes with long simulation times, also with large computationally resources, incompatible with the requirement of simulation of energy plants for long periods.

The one-dimensional model with mixing algorithm presented an additional limit regarding the geometry of the tank as presented in Fig. 1. During the charge phase, hot water enters the lower inlet port of the tank. The mixing algorithm is not triggered for the cold layers below the inlet port leaving the temperature unchanged, with only a little rise due to heat conduction. However, in reality, the water enters with a momentum and a horizontal plume develops, mixing also the water below the inlet port. To override the problem the mixing of the water layers below the inlet port has been forced also in presence of a correct thermal gradient during the charge phase.

5.2. Sensible storage

The sensible storage cooling down experimental data has been used for identifying the parameters of the tank to be used in the following comparison. In order to identify the heat transfer coefficient of the tank, experimental data, obtained during charging and discharging phases, have been used. An identification method has been applied for automatically minimizing the error between the temperatures history of the four levels with recorded history data, obtaining a tank heat loss coefficient of 2.17 W/(m^2 K) comparable with the one obtained with the fully mixed case.

5.3. Test A

The tank component with PCM has then been validated using the experimental results of test A. Fig. 10 reports the time dependent temperature comparison between numerical and experimental results for RT65 at the four-sensor location presented in Fig. 1. The model predicts fairly well the temperature behavior at the beginning of the test with the sudden reduction of temperature due to the flow of cold water. Fig. 11 reports the long-term behavior showing the effect of reheating due to the PCM clearly visible for water temperature T1, the one positioned near the layer with

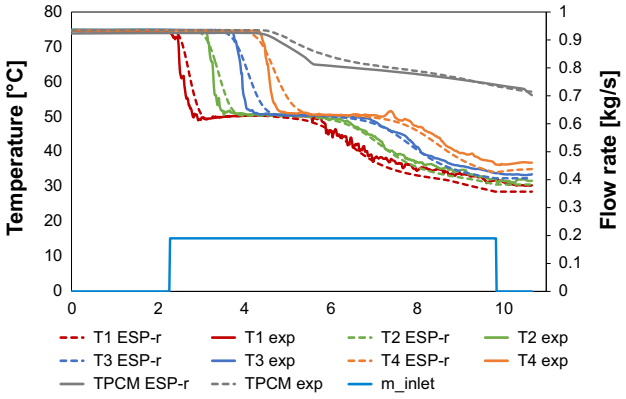

Fig. 10. Test A RT65 16 cylinders, comparison between temperature-time evolutions.

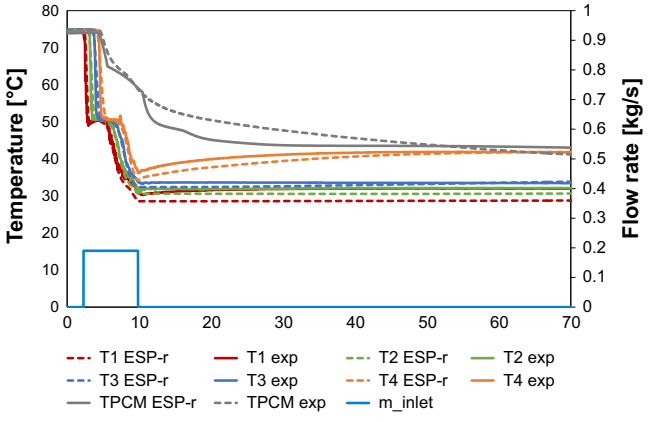

Fig. 11. test A, reheating effect.

PCM modules. In Fig. 11 the numerical PCM temperature is not easily defined since, as declared before, the geometry is quite different and so it is impossible to identify the position in PCM modules corresponding to the experimental measurement point. Nevertheless it can be appreciated the similar behavior during the phase change in which the temperature recovering can be easily identified. Temperature T1, the one positioned in proximity of the inlet at the bottom of the tank, shows the largest difference, higher than the ones of temperatures T2 and T3, furthermore temperature T1 increases also when the cold water inflow stops, and the value reaches the value of temperature T2. This different behavior can be explained by the cold water inflow which creates a mixing recirculating vortex that enhance a mixing between cold and hot water layers. The one-dimensional model of water stratification implemented in ESP-r cannot describe the mixing effect thus the stratification is enhanced. It is worth noting that the design of water tanks in real applications usually provides the water inlet with diffusers in order to allow water stratification and avoiding the formation of large mixing vortices.

5.4. Test B

Fig. 12 reports the time history of water temperature in Test B using 16 cylinders filled with RT65 PCM. During this test, two discharging phases lasting 5 min each are applied. Similar behavior is observed between experimental and numerical tests, with an increase of temperature registered by sensor T4 positioned in the area of the PCM cylinders. It is worth noting that again also the experimental value of T1, the sensor far from the PCM, registers

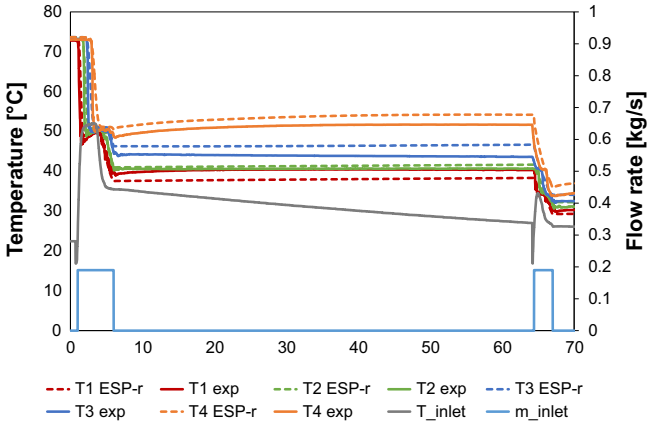

Fig. 12. Test B RT65 16 cylinders, comparison between experimental and numerical temperature-time evolution.

an increase in temperature during both discharge phases. This behavior is not reproduced by the numerical result and can be again explained by the presence of recirculation zones that mix the water between upper hot and cold low zones. As explained before, the numerical approach considers water stratification with a one-dimensional model, which is not capable of dealing with such effects. This behavior explains also the steeper thermocline registered in the numerical results, mixing effects between hot and cold layers reduce the temperature difference between sensors T1 and T4. From a practical point of view the adoption of diffusers at inlet are usually employed in order to reduce recirculation effects and the development of thermal plumes inside tanks enhancing thermal stratification.

6. Conclusions

In the present paper, a study of different hybrid "sensible + latent" heat storage configurations for domestic application is presented.

Different charging and discharging tests have been performed by means of a properly designed test rig, realized in accordance to the standard EN 12977-3, able to simulate real operating conditions of a heat storage for domestic applications.

Two different PCMs have been selected, a commercial paraffin, RT 65, and a hydrate salts mixture, realized in the CNR ITAE lab, having a nominal melting temperature of 58 °C. Different amount of PCMs have been included inside a 48 dm^3 hot water heat storage tank in order to evaluate the possible increasing in energy stored and delivered to the user, by macro-encapsulating the PCM inside small size (80 cm^3) polypropylene capsules.

The experimental results showed an increasing of the hot water delivering capacity to a typical domestic user, compared to the sensible hot water system. In particular, an increasing of about 10% was obtained employing around 1.3 dm^3 of PCM 58. Similar results have been reached employing almost a double volume of RT 65. This outcome is related to the noticeably higher density of the PCM 58 mixture compared to the paraffin RT 65. Moreover, the presence of an evident sub-cooling effect for the PCM 58 seems to have a reduced effect on the overall achievable performance of the system.

Experimental results have been also used for testing a tank model with latent heat storage. The model is an extension of the model implemented in the software ESP-r. The simulations highlighted that the model can accurately reproduce the experimental tests, both for the sensible cooling down test and for Tests A and B for the latent heat storage. The major discrepancies between numerical and experimental data are due to the simplified one dimensional stratification model that is not capable to replicate recirculation areas inside the tank. The numerical model will be enhanced in future to accommodate sub-cooling effects in order to simulate PCM materials sensible to these phenomena.

Acknowledgments

The authors thank Dr. F. Frusteri for the preparation of PCM 58 mixture.

This work was partially supported by Italian Ministry for the Economic Development: "Progetto PIACE, Piattaforma intelligente, Integrata e Adattativa di micro Cogenerazione ad elevata Efficienza per usi residenziali – Industria 2015" [Grant No. 00024EE01].

References

[1] Arteconi A, Hewitt NJ, Polonara F. State of the art of thermal storage for demand-side management. Appl Energy 2012;93:371–89.
[2] Tatsidjodoung P, Le Pierres N, Luo L. A review of potential materials for thermal energy storage in building applications. Renew Sust Energy Rev 2013;18:327–49.
[3] Fath HES. Technical assessment of solar thermal energy storage technologies. Renew Energy 1998;14:35–40.
[4] Mehling H, Cabeza LF, Hippeli S, Hiebler S. PCM-module to improve hot water heat stores with stratification. Renew Energy 2003;28:699–711.
[5] Nabavitabatabayi M, Haghighat F, Moreau A, Sra P. Numerical analysis of a thermally enhanced domestic hot water tank. Appl Energy 2014;129:253–60.
[6] Pielichowska K, Pielichowski K. Phase change materials for thermal energy storage. Prog Mater Sci 2014;65:67–123.
[7] <http://www.rubitherm.de/> [accessed on 26/05/2016].
[8] <http://www.pcmproducts.net/> [accessed on 26/05/2016].
[9] Pereira da Cunha J, Eames P. Thermal energy storage for low and medium temperature applications using phase change materials – a review. Appl Energy 2016;177:227–38.
[10] Mazman M, Cabeza LF, Mehling H, Nogues M, Evliya H, Paksoy HÖ. Utilization of phase change materials in solar domestic hot water systems. Renew Energy 2009;34:1639–43.
[11] Nuytten T, Moreno P, Vanhoudt D, Jespers L, Solé A, Cabeza LF. Comparative analysis of latent thermal energy storage tanks for micro-CHP systems. Appl Therm Eng 2013;59:542–9.
[12] Medrano M, Yilmaz MO, Nogués M, Martorell I, Roca J, Cabeza LF. Experimental evaluation of commercial heat exchangers for use as PCM thermal storage systems. Appl Energy 2009;86:2047–55.
[13] Al-Abidi AA, Mat S, Sopian K, Sulaiman MY, Mohammad AT. Experimental study of melting and solidification of PCM in a triplex tube heat exchanger with fins. Energy Build 2014;68:33–41.
[14] Sciacovelli A, Gagliardi F, Verda V. Maximization of performance of a PCM latent heat storage system with innovative fins. Appl Energy 2015;137:707–15.
[15] Kabbara M, Groulx D, Joseph A. Experimental investigations of a latent heat energy storage unit using finned tubes. Appl Therm Eng 2016. http://dx.doi.org/10.1016/j.applthermaleng.2015.12.080.
[16] Choi DH, Lee J, Hong H, Kang YT. Thermal conductivity and heat transfer performance enhancement of phase change materials (PCM) containing carbon additives for heat storage application. Int J Refrig 2014;42:112–20.
[17] Xiao X, Zhang P, Li M. Effective thermal conductivity of open-cell metal foams impregnated with pure paraffin for latent heat storage. Int J Therm Sci 2014;81:94–105.
[18] Dannemand M, Johansen JB, Kong W, Furbo S. Experimental investigations on cylindrical latent heat storage units with sodium acetate trihydrate composites utilizing supercooling. Appl Energy 2016;177:591–601.
[19] Report of IEA Solar Heating and Cooling programme – Task 32 "Advanced storage concepts for solar and low energy buildings" Report C3 of Subtask C, May 2007 Edited by: Wolfgang Streicher.
[20] Castell A, Solé C, Medrano M, Nogués M, Cabeza LF. Comparison of stratification in a water tank and a PCM-water tank. J Sol Energy – T Asme 2009;131. http://dx.doi.org/10.1115/1.3097277.
[21] Heim D, Clarke JA. Numerical modelling and thermal simulation of PCM–gypsum composites with ESP-r. Energy Build 2004;36:795–805.
[22] Padovan R, Manzan M. Genetic optimization of a PCM enhanced storage tank for solar domestic hot water systems. Sol Energy 2014;103:563–73.
[23] de Gracia A, Oró E, Farid MM, Cabeza LF. Thermal analysis of including phase change material in a domestic hot water cylinder. Appl Therm Eng 2011;31:3938–45.
[24] EN 12977-2:2012. Thermal solar systems and components – custom built systems – Part 3: performance test methods for solar water heater stores.
[25] Doebelin EO. Measurements systems: application and design. 4th ed. Singapore: McGraw-Hill International Editions; 1990.
[26] TRNSYS, A Transient System Simulation Program, Version 17, Solar Energy Laboratory, Univ. of Wisconsin-Madison. <www.trnsys.com>.

[27] Fan J, Furbo S. Buoyancy driven flow in a hot water tank due to standby heat loss. Sol Energy 2012;86:3438–49.
[28] Frusteri F, Leonardi V, Vasta S, Restuccia G. Thermal conductivity measurement of a PCM based storage system containing carbon fibers. Appl Therm Eng 2005;25:1623–33.
[29] Frazzica A, Maggio G, Freni A. Experimental and theoretical analysis of the behaviour of a macro-encapsulated organic compound for solar cooling application. In: Proceedings of INNOSTOCK 2012 - The 12th International Conference on Energy Storage, 16–18 Maggio 2012, Lleida, Spagna.
[30] Clarke JA. Energy simulation in building design. Oxford, GB: Butterworth Heinmann; 2001.
[31] Padovan R, Manzan M. Development of a stratified tank storage component for ESP-r with embedded phase change material modules. J Power Energy 2013;227:53–61.